Neurochemistry International 128 (2019) 39–49

Contents lists available at ScienceDirect

Neurochemistry International

journal homepage: www.elsevier.com/locate/neuint

Exendin-4 attenuates brain mitochondrial toxicity through PI3K/Akt-dependent pathway in amyloid beta (1–42)-induced cognitive deficit rats

Debapriya Garabadu*, Jaya Verma

Division of Pharmacology, Institute of Pharmaceutical Research, GLA University, Mathura, 281 406, India

ARTICLE INFO

Keywords:
Glucagon-like peptide-1
Amyloid beta
Acetylcholine
Mitochondria
Hippocampus
Pre-frontal cortex

ABSTRACT

Alzheimer's disease (AD) is a progressive neurodegenerative disorder characterized by memory loss, disorientation and gradual deterioration of intellectual ability. In the pharmacotherapy of AD, the mitochondrial protective activity of Exendin-4 in experimental studies is yet to be established though its effectiveness is demonstrated in these patients. Therefore, the mitochondria protective activity of Exendin-4 (5 μg/kg, i.p.) was investigated in hippocampus and pre-frontal cortex (PFC) of AD-like animals. The amyloid beta (Aβ) was injected through bilateral intracerebroventricular route into lateral ventricles to induce AD-like manifestations in the male rats. Exendin-4 significantly attenuated Aβ-induced memory-deficits in the Morris water maze and Y-maze test protocols. Exendin-4 significantly decreased Aβ-induced increase in the level of Aβ in both brain regions. Exendin-4 significantly increased Aβ-induced decrease in acetylcholine level and activity of cholineacetyl transferase in all brain regions. Moreover, Exendin-4 significantly decreased Aβ-induced increase in the activity of acetylcholinestrase in both the brain regions. E4 significantly increased Aβ-induced decrease in mitochondrial function, integrity, respiratory control rate and ADP/O in all brain regions. Further, Exendin-4 significantly decreased Aβ-induced increase in the mitochondrial complex enzyme-I, IV and V activities in all brain regions. Furthermore, Exendin-4 significantly increased Aβ-induced decrease in the level of phosphorylated Akt and the ratio of phosphorylated Akt to Akt in both brain regions. However, LY294002 diminished the therapeutic effects of Exendin-4 on behavioral, biochemical and molecular observations in AD-like animals. Pearson's analysis showed that the attributes of mitochondrial dysfunction (MMP and RCR) exhibited significant correlation to the loss in memory formation, level of Aβ and cholinergic dysfunction in these animals. Thus, it can be speculated that Exendin-4 may mitigate AD-like manifestations including mitochondrial toxicity perhaps through PI3K/Akt-mediated pathway in the experimental animals. Hence, Exendin-4 could be a potential therapeutic alternative candidate in the management of AD.

1. Introduction

Alzheimer's disease (AD) is a progressive neurodegenerative disorder characterized by memory loss, disorientation and gradual deterioration of intellectual ability. It has been suggested that AD accounts around 50–60% of all cases of dementia that affects about 50 million people worldwide (Patterson, 2018). The pathophysiology of AD involves depleted levels of brain cholinergic transmitter (Francis et al., 1999), extracellular β-amyloid (Aβ) plaque (Karran et al., 2011), microtubule τ-protein aggregation (Šimić et al., 2016), neuroinflammation and oxidative stress (Agostinho et al., 2010), disruption of calcium homeostasis (Mattson, 2010), dyshomeostasis of bio-metal ions (copper, iron and zinc; Bush, 2013) and many more. Therefore, these divergent pathobiological pathways of AD make it complex and multifactorial neurodegenerative disorder. Moreover, it has been well suggested that a single molecule that has been endowed with a specific target could not be sufficiently effective in the management of AD (Agis-Torres et al., 2014). Hence, multi-target drug approach has to be considered in the pharmacotherapy of AD.

Several therapeutic approaches have been developed to lower or clear Aβ aggregation but they fail to gain anticipated benefits in the clinical trials (Lambert et al., 1998; Mangialasche et al., 2010; Benilova et al., 2012; Giacobini and Gold, 2013; Goure et al., 2014). It has also been demonstrated that impaired cortical cholinergic dysfunction contributes to Aβ aggregation in the pathogenesis of AD (Yan and Feng, 2004). Additionally, both *in vitro* tests and experimental animal studies suggest that the increasing levels of acetylcholine (ACh) with cholinesterase inhibitors decrease Aβ neurotoxicity and slow the progression

* Corresponding author.
E-mail addresses: debapriya.garabadu@gla.ac.in, debapriya.2007@gmail.com (D. Garabadu).

https://doi.org/10.1016/j.neuint.2019.04.006
Received 7 January 2019; Received in revised form 10 April 2019; Accepted 11 April 2019
Available online 17 April 2019
0197-0186/

of AD (Grimaldi et al., 2016). Thus, cholinergic dysfunction and intracellular Aβ accumulation may converge at subcellular level.

Mitochondrial dysfunction in the brains of AD patients correlates with a wide range of mitochondrial abnormalities including mitochondrial DNA defects, reduced mitochondrial electron transport chain activity, mitochondrial adenosine triphosphate (ATP), decreased levels of mitochondrial enzyme activities, impaired mitochondrial trafficking, and increased oxidative stress (Swerdlow et al., 2010; Reddy and Reddy, 2011). Growing researches document that there is an association between the intracellular Aβ cascade and the dysfunction of subcellular organelles especially mitochondria (Du et al., 2008; Dragicevic et al., 2011). It has also been suggested that Donepezil reduces mitochondrial dysfunction in transgenic mice (Ye et al., 2015). These observations clearly demarcate the fact that mitochondrial dysfunction may be a common link to cholinergic dysfunction and Aβ accumulation in the pathophysiology of AD.

It has been demonstrated that glucagon-like peptide-1 (GLP-1) agonists are neuroprotective against cell culture and mouse models of AD (Perry and Greig, 2004; McClean et al., 2011). These agents are considered as growth factors in the brain that facilitates synaptogenesis and neurogenesis, and thus protects against oxidative injury. In AD mouse models, GLP-1 agonists reduce levels of AD pathologic markers, including Aβ level, decrease microglial activation and improve memory formations (McClean et al., 2011). It is well established that GLP-1 can cross the blood-brain barrier and exhibit physiological response in the brain. When GLP-1 bounds to its receptor, it activates signaling pathways that leads to the downstream modulation of cellular proteins including PI3K. Moreover, a randomized, double-blind, placebo-controlled trial suggests that exenatide (Exendin-4) exhibits neuroprotective activity probably through PI3K downstream pathway and can also improve neuronal survival, mitochondria function and neuroinflammation (Athauda et al., 2017).

Hence, in the present study, the neuroprotective activity of Exendin-4 was investigated against mitochondrial toxicity in addition to increased level of Aβ and cholinergic dysfunction in hippocampus (HIP) and PFC of Aβ-induced AD-like rodents. Moreover, the neuroprotective activities of Exendin-4 were evaluated in presence of LY294002, PI3K inhibitor, to establish the downstream pathway of GLP-1 receptor in the modulation of mitochondrial bioenergetics in the above brain regions.

2. Materials and methods

2.1. Animals

Adult male wistar albino rats (180 ± 20 g) of age 6–8 weeks were procured from the central animal house, Institute of Pharmaceutical Research, GLA University, Mathura. The thirty six animals in experimental study were divided into six groups of six each. Rats were housed in poly-acrylic cages at ambient temperature 25 ± 1 °C and of relative humidity 45–55%, with a 12:12 h light/dark cycle. Animals were freely allowed to feed their standard pellet diet (Lipton India, Ltd., Mumbai) and water *ad libitum* during the experiment. The experimental procedures were performed according to the principles of the Institutional Animal Ethics Committee (1260/PO/ERe/S/09/CPCSEA/IAEC/2018/P.Col/R02) under strict compliance of the Committee for the Purpose of Control and Supervision of Experiments on Animals (CPCSEA) guidelines for experimental studies. Further, principles of laboratory animal care (National Research Council (US) Committee for the update of the guide for the care and use of laboratory animals, 2011) have been followed during the experiments.

2.2. Chemicals and reagents

The chemicals such as amyloid beta (1–42; Aβ), TMRM, Exendin-4 (E4), LY294002 and Amplex red assay kit for ACh and AChE were purchased from Sigma (St. Louis, MO, USA). All other analytical grade reagents and chemicals were purchased from Merck Pvt. Ltd., New Delhi.

2.3. Stereotaxic injection of Aβ

The scalp of anesthetized rat (sodium pentobarbital; 40 mg/kg; i.p.) was incised and retracted, and the head was positioned to place bregma and lambda in the same horizontal plane in a stereotaxic frame (Stoelting, USA). Two small holes of 1.5 mm depth were drilled on both sides of lateral cerebral ventricle and stainless-steel guide cannulas were implanted (posterior – 0.8 mm, medial/lateral ± 1.5 mm relative to bregma, dorsal/ventral −3.8 mm below dura; Paxinos and Watson, 1998). Aβ, dissolved in artificial cerebrospinal fluid (aCSF), was injected through Hamilton syringe via polyethylene tube (1 μg/μl, 5 μl/animal; 1.0 μl/min) into each of the lateral cerebral ventricles over a 5 min period with a 5 min of lag between the two injections (Li et al., 2014). In Sham animals five μl of aCSF (147 mM NaCl, 2.9 mM KCl, 1.6 mM $MgCl_2$, 1.7 mM $CaCl_2$ and 2.2 mM dextrose; pH −7.4) was infused in both sides of the lateral cerebral ventricles. All microinjections were done with Quintessential Stereotaxic Injector (Stoelting, USA).

2.4. Experimental protocol

The whole experimental protocol was designed for 14 days (Fig-1). Animals were acclimatized for 7 days and then randomly divided into 6 groups each containing 6 animals namely Control, Sham, Aβ, Aβ + E4, Aβ + E4 + LY294002and Aβ + Donepezil. Aβ (1 μg/μL) was administered on Day-1 (D-1) of experimental schedule to all animals except control and sham group rats (Lin et al., 2009; Chen et al., 2014; Nillert et al., 2017). E4 (5 μg/kg, i.p.; Darsalia et al., 2012), LY294002 (50 μg/kg, i.v.; Liu et al., 2015) and Donepezil (1 mg/kg, i.p.; Eissa et al., 2018) were administered to Aβ + E4, Aβ + E4 + LY294002 and Aβ + Donepezil group animals from D-1 to D-14 of experimental schedule respectively. E4 and Donepezil were administered for 14 consecutive days to evaluate the neuroprotective potential of these drugs in Aβ-induced AD-like rats. The Aβ + E4 + LY294002 group rats received E4 at a time lag of 30 min to LY294002 injection to elaborate the downstream PI3K pathway of E4. Animals of Control group were treated with saline. As the protocol was scheduled for 14 days, Morris water maze (MWM) test was performed for five consecutive days (from D-10 to D-14) to evaluate the learning and memory formation of the animals. Subsequently, Y-maze test was performed on D-14 after 1 h to MWM test paradigm to evaluate the spatial memory formation in the animals. All behavioral parameters were recorded and quantified with ANY-maze™ (Version-4.96, USA) video-tracking system. After behavioral observation animals were sacrificed by decapitation method. The brain was microdissected (Paxinos and Watson, 1998) into HIP and PFC, and stored immediately at −80 °C for biochemical estimation. All the biochemical experiments were repeated twice for reproducibility.

2.5. Assessment of effect of E4 on Aβ-induced cognitive deficits in different models

2.5.1. Morris water maze test paradigm

The standard protocol of MWM test procedure was performed to assess learning and memory function of the animals (Morris, 1984;

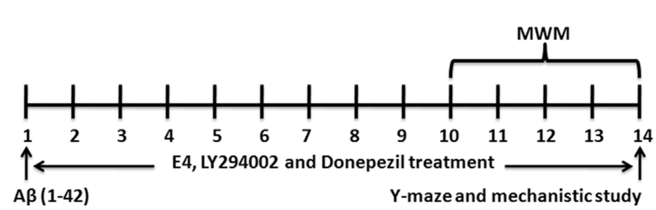

Fig. 1. Diagrammatic representation of detailed experimental schedule.

Pandey and Garabadu, 2017). Briefly, task includes a circular tank painted whole through black and filled with water at the level of 30 cm. Diameter and height of tank was 150 cm and 60 cm respectively. Temperature of tank water was maintained at 27 ± 1 °C. Pool was divided into four equal quadrants. A hidden platform of 4.5 cm in diameter was formed in the middle portion of target quadrant and settled 1.5 cm beneath the upper layer of water. Action of animals was recorded through a video tracking system placed over the water tank. Randomly rats were positioned in the water tank in any one of the quadrants for 120 s and made them free to swim and find out the hidden platform. If animals were unable to find out the platform then they were trained to grasp the platform. The escape latency to find out the hidden platform of all groups of animals was observed and the time taken to find out the platform was recorded by the software. Each rat was placed four times between the gaps of 5 min in each trial to observe the escape latency of them. On fifth day, the hidden platform was removed from the tank. Time spent in each quadrant and time spent in the target quadrants to find out hidden platform was noted down. Percentage of total distance travelled in target quadrant and swimming speed of all groups of animals was also noted down. Time spent in target quadrant was considered as mark of memory rejuvenation.

2.5.2. Y-maze test paradigm

The working memory was determined by observing spontaneous alteration behavior (SAB) through Y-maze test paradigm (Mouri et al., 2007). Test was conducted on last day (14th) of experimental protocol. Y-maze apparatus includes 3 arms (40 cm long and 3 cm wide, with walls 12 cm high) painted whole through black color (named as A, B, C) disposed at 120° apart. Rat was positioned at midpoint of the apparatus and made them free to move. Total number of arm entries and sequences of consecutive entries (ABC, CAB, or BCA, but not BAB) were recorded for 8 min. Arms were wiped throughout the trails to remove resting odor. The percentage alteration behavior was calculated using equation, % spontaneous alteration behavior = [(total number of alternations)/(total number of arm entries − 2)] × 100.

2.6. Evaluation of effect of E4 on cholinergic system

2.6.1. Preparation of the samples

The HIP and PFC tissues were subjected to homogenization in a homogenizer in presence of 1 ml of 0.1 M perchloric acid. The homogenate was collected in a polypropylene tube 50 µl of 4 M potassium acetate was added to adjust the pH to 4.0. Subsequently, the homogenate was subjected to centrifugation for 15 min at 4000 × *g* (Muthuraju et al., 2009).

2.6.2. Assay of activity of ChAT

An enzyme-linked immunosorbent assay kit (SEB929Mu; Wuhan, Hubei, China) was used to quantify the activity of ChAT in a spectrophotometric method at 450 nm as per the instructions of the manufacturer. The results were expressed as n mol/hr/mg protein.

2.6.3. Analysis of ACh level

Amplex red assay kit (Molecular Probes, Inc., USA) was used to estimate the amount of ACh in brain tissue as per standard protocol of Zoukhri and Kublin (2001). Briefly, 0.1 ml of control (10 µM H_2O_2) and tissue homogenate were collected in two separate polypropylene tubes. Subsequently, 0.1 ml of assay buffer (50 mM Tris–HCl, pH 7.5) containing 0.2 M Amplex red reagent, 2 U/ml horseradish peroxidase, 0.2 U/ml choline oxidase and 10 U/ml AChE was added to each tube. The fluorescence was recorded with the help of spectrofluorometer at 530 nm excitation and 590 nm emission wavelengths after 45 min of incubation period. The protein content was determined as per standard protocol of Lowry et al. (1951).

2.6.4. Estimation of activity AChE in different brain regions

The Amplex red AChE assay kit (Molecular Probes, Inc., USA) was used to estimate the activity of AChE in discrete brain regions. Briefly, 0.1 ml of standard AChE (0.2 U/ml), control (10 µM H_2O_2) and tissue homogenate were placed in separate polypropylene tubes. Thereafter, 0.1 ml of assay buffer (50 mM Tris–HCl, pH 7.5) containing 400 µM Amplex Red reagent, 2 U/ml horseradish peroxidase, 0.2 U/ml choline oxidase, and 100 µM acetylcholine was added to each tube and was incubated for 30 min. After incubation, the fluorescence was reported with the help of spectrofluorometer at 530 nm excitation wavelength and 590 nm emission wavelengths. The protein content was determined using standard protocol (Lowry et al., 1951).

2.7. Assessment of effect of E4 on Aβ-induced brain mitochondrial dysfunction

2.7.1. Isolation of mitochondria from discrete rat brain tissues

The standard protocol of Pedersen et al. (1978) was used to isolate the mitochondria from each tissue. The mitochondrial protein content was estimated in each tissue fraction using standard method of Lowry et al. (1951).

2.7.2. Estimation of mitochondrial function

The (3-(4, 5-dimethylthiazol-2-yl)-2,5diphenyltetrazolium bromide; MTT) reduction assay was considered to assess mitochondrial function in each tissue fraction in terms of estimating the level of formazan formed using spectrophotometric method at 595 nm wavelength (Kamboj et al., 2008). The results were expressed as mg formazan formed/min/mg protein.

2.7.3. Evaluation of MMP in discrete brain regions

The MMP was estimated in terms of the extent of rhodamine dye taken up by mitochondria was measured in spectrofluorometer (Hitachi, F-2500) at an excitation λ of 535 ± 10 nm and emission λ of 580 ± 10 nm (Huang, 2002). The results were expressed as fluorescence intensity/mg protein.

2.7.4. Estimation of mitochondrial bioenergetics

Clark oxygen electrode (Hansatech Instruments Pvt. Ltd., USA) was used to monitor the extent of mitochondrial respiration using principle of polarography. 1 mg/ml of isolated mitochondria preparation was incubated in a respiratory medium containing 125 mM sucrose, 65 mM KCl, 2.5 mM $MgCl_2$, 5 mM KH_2PO_4, 5 mM Hepes, pH 7.2 at 30 °C. An initial rate of oxygen consumption (state 2 orV_2) was recorded after addition of pyruvate plus malate (10 mM/5 mM). Subsequently, the state 3 rate (V_3) was recorded after addition of 250 nmol of ADP. Thereafter, a measurable state 4 rate (V_4) (i.e., the rate after ADP phosphorylation) was monitored when a second pulse of ADP was added but the phosphorylative cycle was soon inhibited before its completion by adding 1 µg of oligomycin. Subsequently, a measurable oligomycin oxygen consumption rate (V_{olig}) was obtained after 1 µM concentration of the uncoupling agent FCCP was added to obtain a rate of oxygen consumption in the absence of coupled oxidative phosphorylation (V_{FCCP}). Further, the oxygen consumption was recorded in presence of 15 mM succinate and 2.2 mM rotenone to elaborate the respiratory complex-II activity. Respiratory control ratios (RCR) and ADP/O were determined according to the standard protocol of Chance and Williams (1956).

2.7.5. Estimation of mitochondrial respiratory complex-I, II, IV and V activity

The principle of catalytic oxidation of NADH with potassium ferricyanide was used to estimate the activity of NADH dehydrogenase (complex-I) in different mitochondrial fractions at excitation wavelength of 350 nm and emission wavelength of 470 nm for NADH (Shapiro et al., 1979). The NADH dehydrogenase activity was expressed

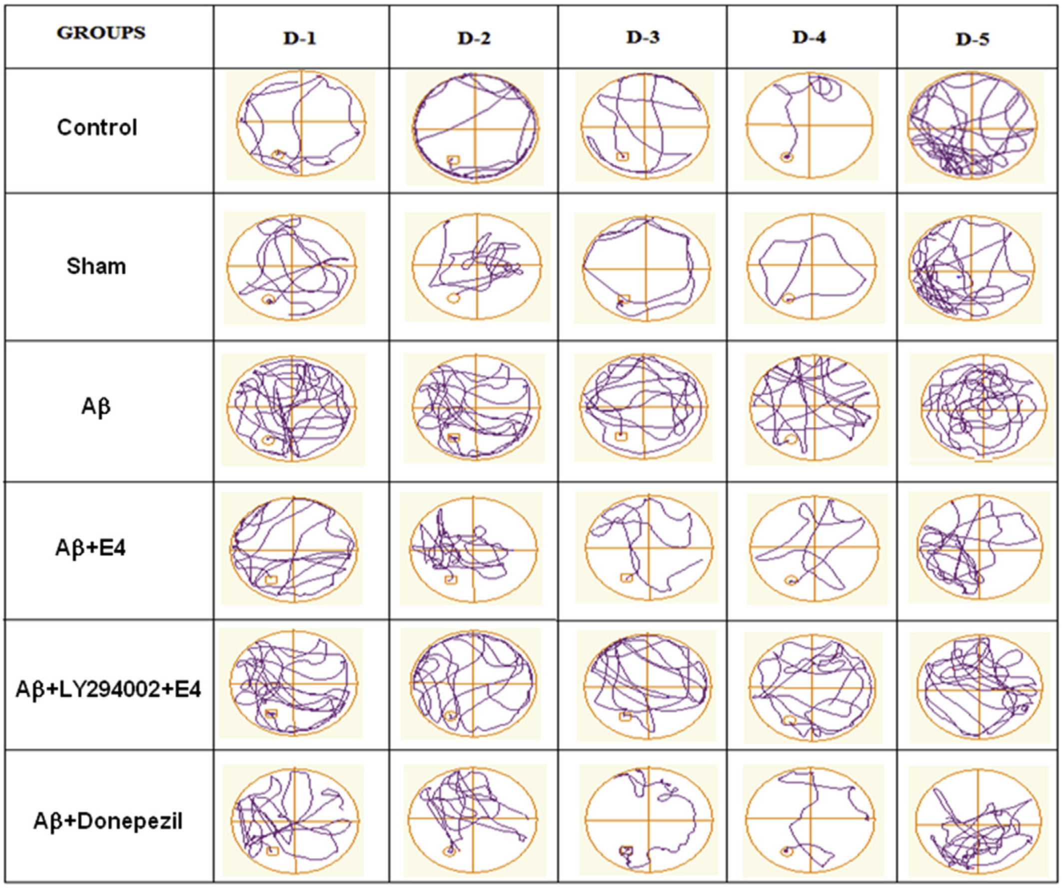

Fig. 2. Representative tracking plot of each animal of each group on all days in Morris water maze test protocol.

as nmole NADH oxidized/min/mg protein. The principle of progressive reduction of nitro blue tetrazolium (NBT) to an insoluble colored compound, diformazan was employed to determine the activity of mitochondrial succinate dehydrogenase (SDH; complex-II) at 570 nm in different sample preparations (Sally and Margaret, 1989). The SDH activity was expressed as micromole formazan produced/min/mg protein. The activity of cytochrome oxidase (complex-IV) was determined in different mitochondrial fraction in presence of reduced cytochrome *c* at 550 nm for 3 min (Storrie and Madden, 1990). Results were expressed as nmole cytochrome *c* oxidized/min/mg protein (ε_{550} = 19.6 $mmol^{-1}cm^{-1}$). The F1−F0 synthase (complex-V) was estimated by incubating mitochondrial preparation in the presence of ATPase buffer (Griffiths and Houghton, 1974) and the content of phosphate was monitored (Fiske and Subbarao, 1925). Results were expressed as nmole ATP hydrolyzed/min/mg protein.

2.8. Estimation of cytosolic Aβ

The level of Aβ was determined spectrophotometrically at 450 nm using an enzyme-linked immunosorbent assay kit (ArigoBiolaboratories, Taiwan; ARG80939) according to the manufacturer's instructions.

2.9. Western blot analysis

Briefly, the HIP and PFC were lysed in buffer containing complete protease inhibitor cocktail. Protein concentrations were determined according to standard method (Bradford, 1976). A standard plot was generated using bovine serum albumin. An aliquot of each sample was electrophoresed in 10% SDS PAGE gels for Akt and pAkt proteins, transferred to polyvinylidene fluoride membranes. The membranes were incubated in blocking buffer: phosphate-buffered saline (PBS) containing 5% milk for 1 h at room temperature, and thereafter probed overnight at 4 °C with specific primary antibodies diluted in PBS with 2.5% milk and 0.1% Tween 20. The membrane was incubated overnight with rabbit anti-Akt (1:1000; Abcam Plc., Cambridge, USA), anti-pAkt (1:1000; Abcam Plc., Cambridge, USA) polyclonal primary antibody. After detection with the desired antibodies against the proteins of interest, the membrane was stripped with stripping buffer (25 mMglycine pH 2.0, 2% SDS for 30 min at room temperature) and reprobed overnight with rabbit anti-β-actin polyclonal primary antibody at a dilution of 1:500 to confirm equal loading of protein. Further, membrane was probed with corresponding secondary antibodies. Immunoreactive band of proteins was detected by chemiluminescence using enhanced chemiluminescence (ECL) reagents (Amersham Bioscience, USA). Quantification of the results was performed by densitometric scan of films. The immunoreactive area was determined by densitometric analysis using Biovis gel documentation software.

2.10. Data analysis

All the data were mean ± standard error of the mean (SEM). The escape latency of the animals on day-1 to 4 during MWM test paradigm was analyzed using repeated measure two-way analysis of variance (ANOVA) followed by Bonferroni Post-hoc test. All other statistical analyses of data were performed using one-way ANOVA with Newman-Keuls Post-hoc test to monitor significance among groups. $P < 0.05$ was considered as significant. Further, Pearson's correlation analysis was performed to correlate between MMP and mitochondrial RCR of HIP and PFC and memory loss in MWM (Time spent in target quadrant on Day-5) and Y-maze (% SAB) test protocol. Moreover, Pearson's correlation analysis was performed to correlate between MMP and

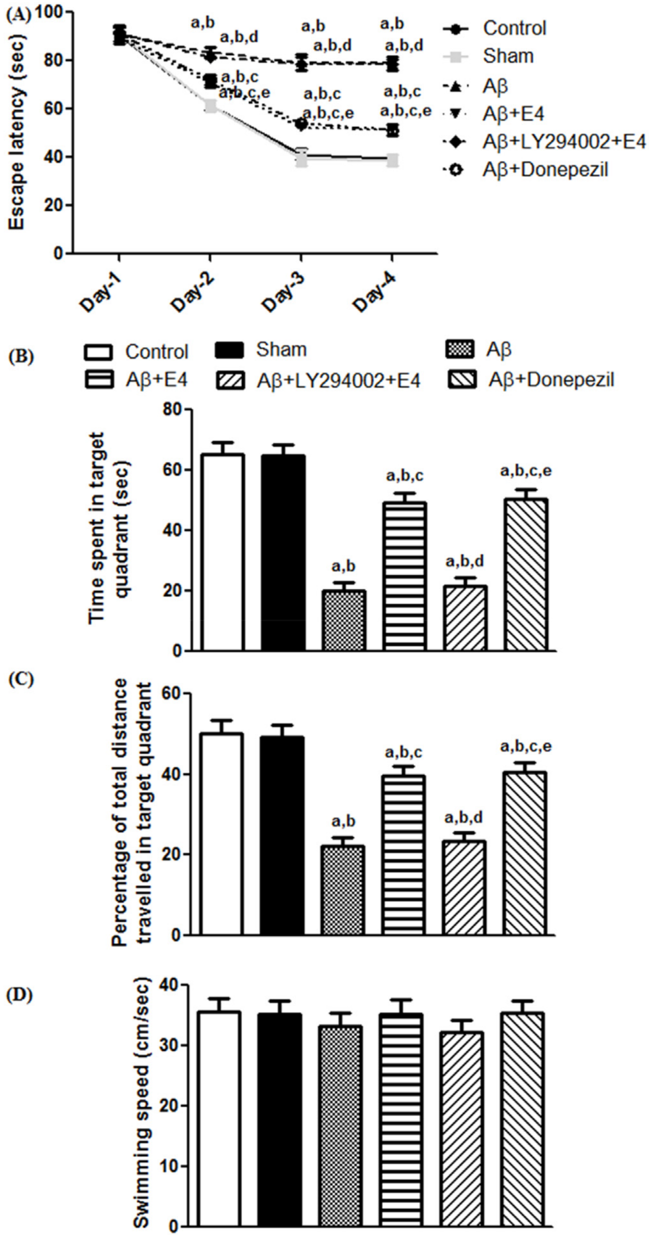

Fig. 3. Effect of Exendine-4 (E4) on amyloid beta (Aβ)-induced changes in the period of escape latency from Day-1 to Day- 4 (A), the time spent in the target quadrant (B), percentage of total distance travelled in target quadrant (C) and swimming speed of the animals (D) in Day-5 of Morris water maze test protocol. All values are Mean ± Standard Error of Mean (SEM; N = 6). ^{a}P < 0.05 compared to Control, ^{b}P < 0.05 compared to Sham, ^{c}P < 0.05 compared to Aβ, ^{d}P < 0.05 compared to Aβ+E4 and ^{e}P < 0.05 compared to Aβ+LY294002 + E4 (Two-way ANOVA followed by Bonferroni Post-hoc test for period of escape latency from Day-1 to Day-4 and for other parameters one-way ANOVA followed by Student Newmann Keuls Post-hoc test).

mitochondrial RCR, amyloid beta and cholinergic dysfunction in each rat brain regions. In correlation analysis the criterion for statistical significance was $P < 0.05$.

3. Results

3.1. E4 ameliorates Aβ (1–42)-induced memory deficits in MWM task in rats

Fig-2 depicts the day-wise representative tracking plot of each animal of each group during the MWM test protocol. Fig-3 illustrates the effect of E4 on spatial learning ability in terms of the period of escape latency in Day-1 to Day- 4 (A) and on spatial memory ability in terms of the time spent in the target quadrant (B), percentage of total distance travelled in target quadrant (C) and swimming speed of the Aβ-challenged animals (D) in Day-5 of MWM test protocol. Statistical analysis revealed that there were significant differences in the escape latency among group [$F (5, 120) = 81.0$, $P < 0.05$] and day [$F (3, 120) = 246.2$, $P < 0.05$]. Further, there was a significant interaction between group and day in the escape latency of the animals [$F (15, 120) = 11.4$, $P < 0.05$]. Post-hoc test showed that there were no significant differences in escape latency of the animals among group on Day-1. E4 significantly reduced the Aβ-induced increase in the escape latency of the animals in Day-2 of the MWM test protocol similar to that of Donepezil. However, LY294002 diminished the therapeutic effect of E4 against Aβ-induced increase in the escape latency of the animals on Day-2 during MWM test paradigm. The observations reported on Day-2 were consistent on Day-3 and 4 of the MWM test protocol.

Statistical analysis revealed that there were significant differences in the time spent in the target quadrant [$F (5, 30) = 38.0$, $P < 0.05$] and percentage of total distance travelled in target quadrant [$F (5, 30) = 22.7$, $P < 0.05$] of the animals in Day-5 of MWM test paradigm. However, there were no significant difference in swimming speed [$F (5, 30) = 0.4$, $P > 0.05$] of the animals among groups. Post-hoc test showed that E4 significantly attenuated the Aβ-induced decrease in the amount of time spent and percentage of total distance travelled in target quadrant of the animals in Day-5 of the MWM test protocol similar to that of Donepezil. However, LY294002 diminished the therapeutic effect of E4 against Aβ-induced decrease in the amount of time spent and percentage of total distance travelled in target quadrant of the animals in Day-5 of the MWM test protocol.

3.2. E4 attenuates Aβ-induced working memory deficits in Y-maze test in rats

Effect of E4 on spatial memory in terms of SAB of the Aβ-challenged animals in Y-maze test protocol is illustrated in Fig-4. Statistical analysis revealed that there were significant differences in the SAB [$F (5, 30) = 29.4$, $P < 0.05$] of the animals among groups. Post-hoc test showed that E4 significantly increased the Aβ-induced decrease in the SAB of the animals during Y-maze test protocol similar to that of Donepezil. However, LY294002 diminished the therapeutic effect of E4 against Aβ-induced decrease in the SAB of the animals during Y-maze test protocol.

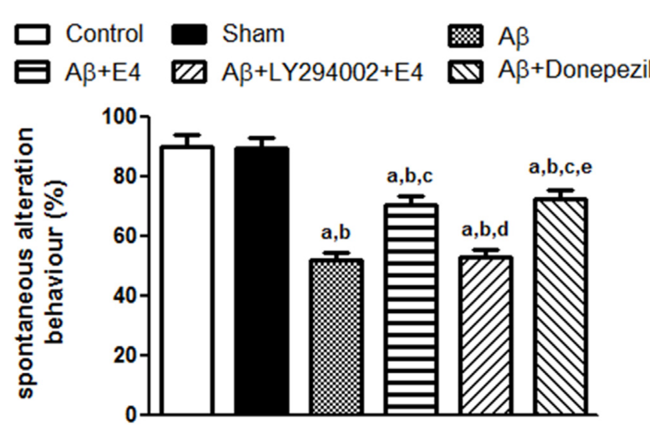

Fig. 4. Effect of E4 on Aβ-induced changes in spatial memory in terms of spontaneous alternation behavior (SAB) of the animals in Y-maze test paradigm. All values are Mean ± SEM (N = 6). ^{a}P < 0.05 compared to Control, ^{b}P < 0.05 compared to Sham, ^{c}P < 0.05 compared to Aβ, ^{d}P < 0.05 compared to Aβ+E4 and ^{e}P < 0.05 compared to Aβ+LY294002 + E4 (One-way ANOVA followed by Student Newmann Keuls Post-hoc test).

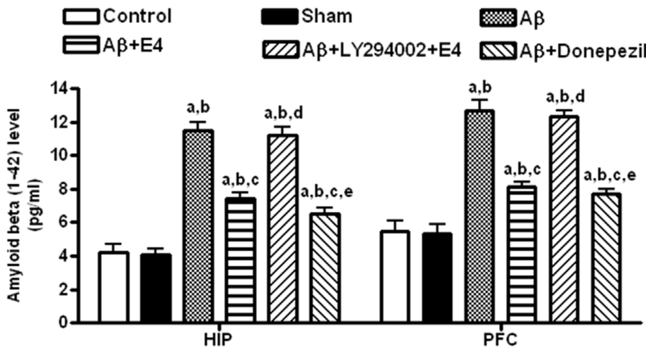

Fig. 5. Effect of E4 on Aβ-induced changes in the level of Aβ in hippocampus (HIP) and pre-frontal cortex (PFC) of the rodents. All values are Mean ± SEM (N = 6). [a]$P < 0.05$ compared to Control, [b]$P < 0.05$ compared to Sham, [c]$P < 0.05$ compared to Aβ, [d]$P < 0.05$ compared to Aβ+E4 and [e]$P < 0.05$ compared to Aβ+LY294002 + E4 (One-way ANOVA followed by Student Newmann Keuls Post-hoc test).

3.3. E4 attenuates Aβ-induced accumulation of Aβ in rat HIP and PFC

Effect of E4 on the level of Aβ in HIP and PFC of the Aβ-challenged rodents is illustrated in Fig-5. Statistical analysis revealed that there were significant differences in the level of Aβ in rat HIP [$F(5, 30) = 54.9$, $P < 0.05$] and PFC [$F(5, 30) = 44.0$, $P < 0.05$] among groups. Post-hoc test showed that E4 significantly decreased the Aβ-induced increase in the level of Aβ in the both regions of the animals similar to that of Donepezil. However, LY294002 diminished the therapeutic effect of E4 against Aβ-induced increase in the level of Aβ in both the rat brain regions.

3.4. E4 improves cholinergic activity in HIP and PFC ofAβ (1–42)-induced cognitive deficit rats

Fig-6 depicts the effect of E4 on the level of ACh (A) and activities of ChAT (B) and AChE (C) in Aβ-challenged rat HIP and PFC. Statistical analysis revealed that there were significant differences in the level of ACh and activities of ChAT and AChE in HIP ([$F(5, 30) = 20.0$, $P < 0.05$], [$F(5, 30) = 30.7$, $P < 0.05$] and [$F(5, 30) = 18.2$, $P < 0.05$] respectively) and PFC ([$F(5, 30) = 22.0$, $P < 0.05$], [$F(5, 30) = 83.5$, $P < 0.05$] and [$F(5, 30) = 15.5$, $P < 0.05$] respectively) among groups. Post-hoc analysis showed that E4 significantly increased the Aβ-induced decrease in ACh level and activity of ChAT in all the rat brain regions. Moreover, E4 significantly decreased the Aβ-induced increase in the activity of AChE in both the rat brain regions. However, LY294002 administration diminished the therapeutic effect of E4 against Aβ-induced changes in the level of ACh and activities of ChAT and AChE in all brain regions of the animals.

3.5. E4 attenuates Aβ (1–42)-induced decrease in mitochondrial function and integrity in discrete rat brain regions

Effect of E4 on the mitochondrial function in terms of the level of formazan produced in MTT assay (A) and integrity in terms of the fluorescence intensity of TMRM (B) in Aβ-challenged rat HIP and PFC are illustrated in Fig-7. Statistical analysis revealed that there were significant differences in mitochondrial function and integrity in HIP ([$F(5, 30) = 43.9$, $P < 0.05$] and [$F(5, 30) = 27.5$, $P < 0.05$] respectively) and PFC ([$F(5, 30) = 44.4$, $P < 0.05$] and [$F(5, 30) = 27.2$, $P < 0.05$] respectively). Post-hoc analysis showed that E4 significantly increased the Aβ-induced decrease in mitochondrial function and integrity in all the rat brain regions. However, LY294002 administration diminished the therapeutic effect of E4 against Aβ-induced decrease in the mitochondrial function and integrity in both rat brain regions.

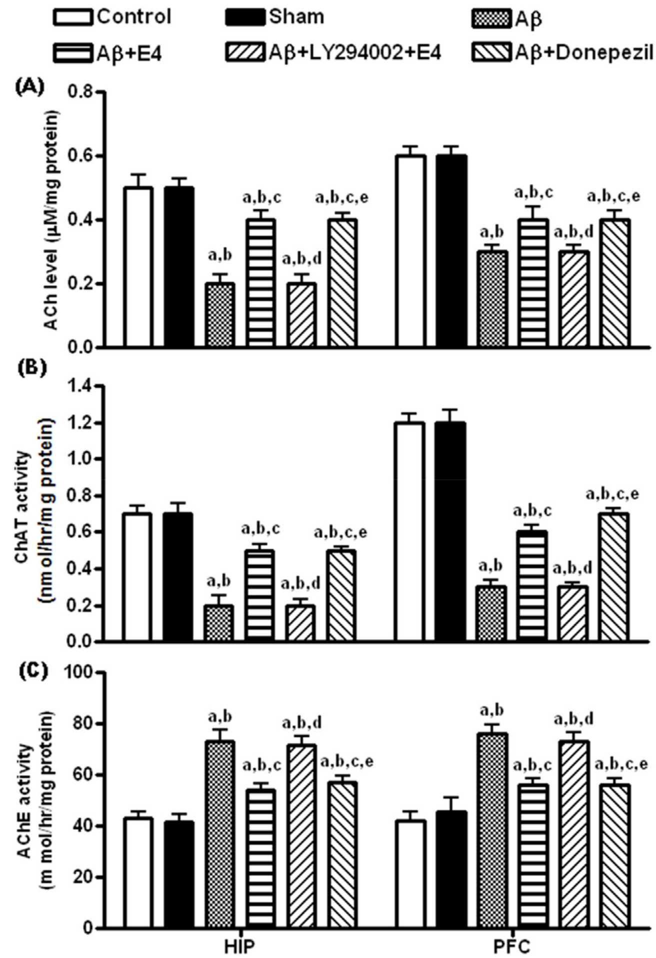

Fig. 6. Effect of E4 on Aβ-induced changes in the level of ACh (A) and activities of ChAT (B) and AChE (C) in rat HIP and PFC. All values are Mean ± SEM (N = 6). [a]$P < 0.05$ compared to Control, [b]$P < 0.05$ compared to Sham, [c]$P < 0.05$ compared to Aβ, [d]$P < 0.05$ compared to Aβ+E4 and [e]$P < 0.05$ compared to Aβ+LY294002 + E4 (One-way ANOVA followed by Student Newmann Keuls Post-hoc test).

3.6. E4 ameliorates Aβ (1–42)-induced decrease in mitochondrial RCR and ADP/O in rat HIP and PFC

Fig-8 depicts the changes in the level of oxygen consumption in different stages of Oxygraph in HIP (A) and PFC (B) of a representative animal of each group of the experimental design. Effect of E4 on the mitochondrial RCR (A) and ADP/O (B) in Aβ-challenged rat HIP and PFC is depicted in Fig-9. Statistical analysis revealed that there were significant differences in mitochondrial RCR and ADP/O in HIP ([$F(5, 30) = 15.1$, $P < 0.05$] and [$F(5, 30) = 36.7$, $P < 0.05$] respectively) and PFC ([$F(5, 30) = 17.3$, $P < 0.05$] and [$F(5, 30) = 25.6$, $P < 0.05$] respectively). Post-hoc analysis showed that E4 significantly increased the Aβ-induced decrease in mitochondrial RCR and ADP/O in all the rat brain regions. However, LY294002 administration attenuated the therapeutic effect of E4 against Aβ-induced decrease in the mitochondrial RCR and ADP/O in all rat brain regions.

3.7. E4 ameliorates Aβ (1–42)-induced changes in mitochondrial complex enzyme activities in rat HIP and PFC

Effect of E4 on the mitochondrial complex enzyme-I, II, IV and V in HIP and PFC of Aβ-challenged animals is illustrated in Table-1. Statistical analysis revealed that there were significant differences in mitochondrial complex enzyme-I, II, IV and V in HIP ([$F(5, 30) = 18.0$,

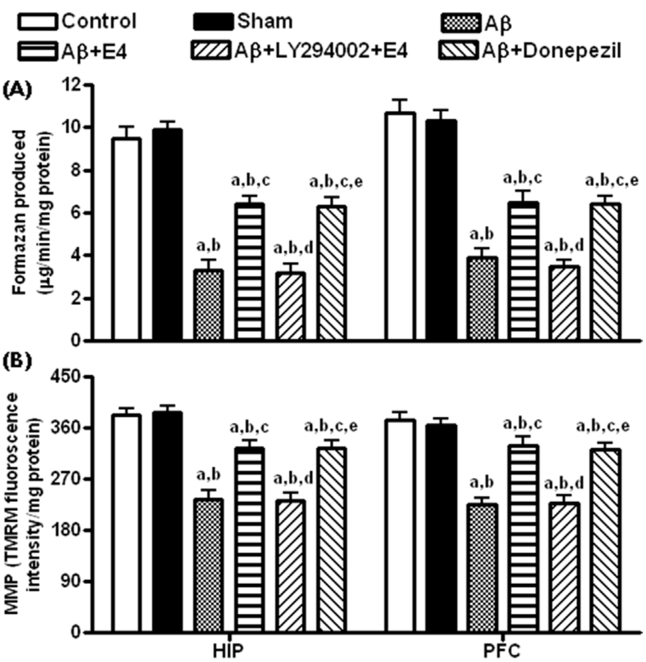

Fig. 7. Effect of E4 on Aβ-induced changes in the mitochondrial function in terms of the level of formazan produced in MTT assay (A) and integrity in terms of the fluorescence intensity of TMRM (B) in rat HIP and PFC. All values are Mean ± SEM (N = 6). $^{a}P < 0.05$ compared to Control, $^{b}P < 0.05$ compared to Sham, $^{c}P < 0.05$ compared to Aβ, $^{d}P < 0.05$ compared to Aβ + E4 and $^{e}P < 0.05$ compared to Aβ + LY294002 + E4 (One-way ANOVA followed by Student Newmann Keuls Post-hoc test).

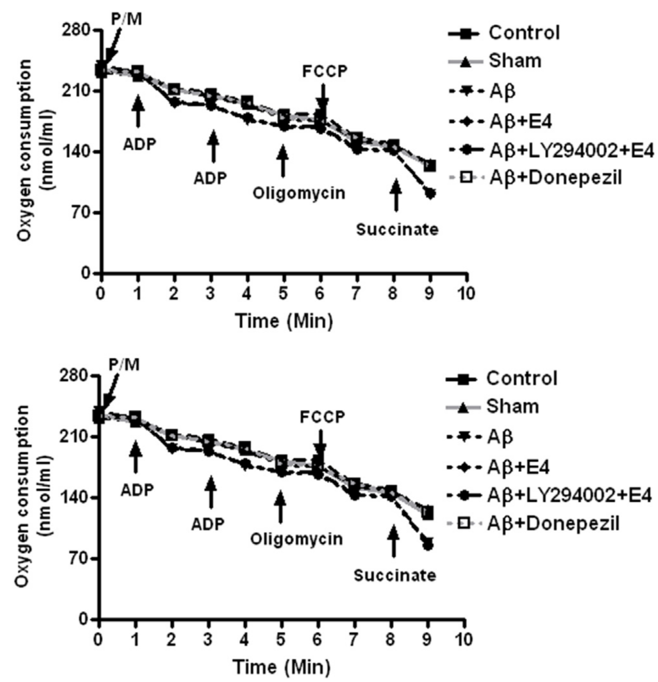

Fig. 8. Representative Oxygraph of HIP (A) and PFC (B) of an animal in each group of the experimental protocol to show the level of oxygen consumption in different stages of mitochondrial respiration. Briefly, at first the initial rate of oxygen consumption (state 2 orV_2) was recorded after addition of pyruvate plus malate (10 mM/5 mM). Further, the state 3 rate of oxygen consumption was recorded after addition of ADP (250 nmol). Moreover, a measurable state 4 rate of oxygen consumption (i.e., the rate after ADP phosphorylation) was monitored when a second pulse of ADP was added but the phosphorylative cycle was soon inhibited before its completion by adding oligomycin (1 µg). Subsequently, a measurable oligomycin oxygen consumption rate was recorded after FCCP (1 µM) was added to obtain a rate of oxygen consumption in the absence of coupled oxidative phosphorylation. Further, the oxygen consumption was recorded in presence of succinate (15 mM) and rotenone (2.2 mM) to observe the respiratory complex-II activity.

$P < 0.05$], [$F (5, 30) = 15.2$, $P < 0.05$], [$F (5, 30) = 20.3$, $P < 0.05$] and [$F (5, 30) = 43.0$, $P < 0.05$] respectively) and PFC ([$F (5, 30) = 17.2$, $P < 0.05$], [$F (5, 30) = 11.2$, $P < 0.05$], [$F (5, 30) = 32.7$, $P < 0.05$] and [$F (5, 30) = 27.0$, $P < 0.05$] respectively). Post-hoc analysis showed that E4 significantly decreased the Aβ-induced increase in the mitochondrial complex enzyme-I, IV and V activities in all the rat brain regions similar to that of Donepezil. However, LY294002 administration attenuated the therapeutic effect of E4 against Aβ-induced increase in the mitochondrial complex enzyme-I, IV and V activities in both rat HIP and PFC.

3.8. E4 ameliorates Aβ (1–42)-induced decrease in phosphorylation of Akt in rat HIP and PFC

Fig-10illustrates the effect of E4 on the levels of expression of Akt (C) and pAkt (D), and ratio of pAkt to Akt (E) in Aβ-challenged rat HIP and PFC. Statistical analysis revealed that there were significant differences in the level of expression of pAkt and ratio of pAkt to Akt in rat HIP ([$F (5, 30) = 43.0$, $P < 0.05$] and [$F (5, 30) = 37.9$, $P < 0.05$] respectively) and PFC ([$F (5, 30) = 65.7$, $P < 0.05$] and [$F (5, 30) = 55.7$, $P < 0.05$] respectively). However, there were no statistical significance in the level of expression of Akt in rat HIP [$F (5, 30) = 1.2$, $P > 0.05$] and PFC [$F (5, 30) = 2.3$, $P > 0.05$]. Post-hoc analysis showed that E4 significantly increased the Aβ-induced decrease in the level of expression of pAkt and the ratio of pAkt/Akt in all the rat brain regions similar to that of Donepezil. However, LY294002 administration attenuated the therapeutic effect of E4 against Aβ-induced decrease in the level of expression of pAkt and the ratio of pAkt/Akt in rat HIP and PFC.

3.9. Correlation analysis between mitochondrial dysfunction and memory loss, Aβ level and cholinergic dysfunction

Table-2 depicts the correlation analysis of mitochondrial dysfunction of each brain region and memory loss in MWM and Y-maze tests. A significant positive correlation was observed between MMP of HIP and PFC, and time spent in target quadrant in MWM test and percentage of SAB in Y-Maze test. Similarly, a significant positive correlation was observed between mitochondrial RCR of HIP and PFC, and time spent in target quadrant in MWM test and percentage of SAB in Y-Maze test. Further, there was a negative correlation between MMP and level of Aβ and activity of AChE in both HIP and PFC. Moreover, there was also a negative correlation between mitochondrial RCR and level of Aβ and activity of AChE in both the brain regions. Furthermore, a significant positive correlation was observed between MMP and level of ACh and activity of ChAT in HIP and PFC. Additionally, there was also a significant positive correlation between mitochondrial RCR and level of ACh and activity of ChAT in HIP and PFC.

4. Discussion

The present study demonstrates for the first time that Exendin-4 attenuated mitochondrial toxicity in HIP and PFC of Aβ-induced AD-like rodents. In addition, Exendin-4 reduced Aβ level and cholinergic dysfunction in the above brain regions of AD-like rats. Moreover, Exendin-4 reduced memory impairment in AD-like animals. However, LY-294002 diminished the therapeutic effects of Exendin-4 on behavioral, biochemical and molecular observations in AD-like animals. These observations clearly indicate that Exendin-4 mitigates AD-like manifestations perhaps through PI3K-mediated pathway in the animals.

In the present study Exendin-4 substantially attenuated Aβ-induced

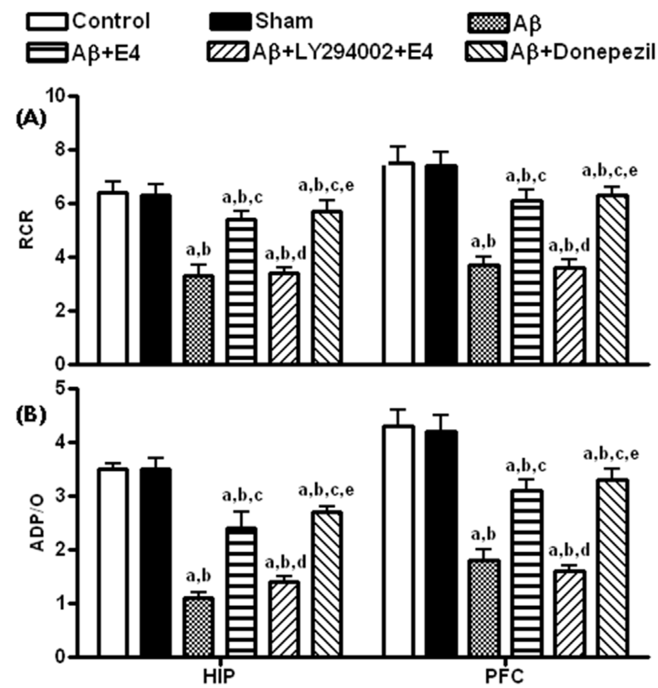

Fig. 9. Effect of E4 on Aβ-induced changes in the mitochondrial respiratory control ratio (RCR; A) and ADP/O (B) in rat HIP and PFC. All values are Mean ± SEM (N = 6). $^{a}P < 0.05$ compared to Control, $^{b}P < 0.05$ compared to Sham, $^{c}P < 0.05$ compared to Aβ, $^{d}P < 0.05$ compared to Aβ+E4 and $^{e}P < 0.05$ compared to Aβ+LY294002 + E4 (One-way ANOVA followed by Student Newmann Keuls Post-hoc test).

memory impairments in MWM and Y-maze paradigms similar to that of earlier reports (Jia et al., 2016; Wang et al., 2016). Moreover, Exendin-4 significantly attenuated Aβ level in the memory-sensitive brain regions of AD-like rodents. In this context, it has been reported that Exendin-4 attenuated Aβ level and elevated level of amyloid precursor protein in the Aβ-challenged hippocampal neurons (Perry et al., 2003). Li et al. (2010) further supported the fact that Exendin-4 attenuated Aβ level in the brain of streptozotocine-treated transgenic AD mice. Moreover, the present study also reported that Exendin-4 attenuated Aβ-induced cholinergic dysfunction in the memory-sensitive brain regions of AD-like animals. It has been well documented that the depleted presynaptic cholinergic markers in the cerebral cortex (Bowen et al., 1976) and deteriorated nucleus basalis of Meynert in the basal forebrain which is the source of cortical cholinergic innervations (Whitehouse et al., 1981) are supporting evidences to the cholinergic hypothesis of AD. Among several ways to ameliorate the symptoms of AD through cholinergic treatment, the most effective one is by using cholinesterase inhibitors (Summers et al., 1986). The present study reported that Exendin-4 attenuated Aβ-induced increase in AChE activity in both the brain regions similar to that of Donepezil. Further, the present study also revealed that Exendin-4 attenuated Aβ-induced decrease in ACh level and ChAT activity in both the brain regions. It has been suggested from the experimental studies that the increased level of Aβ impairs pyruvate dehydrogenase activity by activating mitochondrial tau protein kinase I/glycogen synthase kinase-3 beta and thus provides inadequate supply of acetyl-CoA in the synthetic pathway of ACh in the neurons (Hoshi et al., 1997), indicating the potential contribution of Exendin-4 on mitochondrial function in both the brain regions. Furthermore, the increased level of Aβ is another cause for the mitochondrial dysfunction in AD brains (Devi et al., 2006). These observations clearly demonstrate that Exendin-4 attenuates mitochondrial dysfunction that perhaps common to elevated level of Aβ and cholinergic dysfunction in the AD-like animals.

Mitochondrial impairment and loss plays a critical role in neuronal degeneration and disease progression in AD. Damaged mitochondria are less bioenergetically efficient and produce detrimental structural and functional consequences for the AD neurons (Onyango, 2018). In the present study it has been demonstrated that mitochondrial function and integrity were reduced in both the brain regions of AD-like animals. Moreover, Aβ administration caused increased activities of complex-I, II, IV and V of mitochondrial electron transport chain (ETC) similar to that of earlier report (Simoncini et al., 2015). Subsequently, there was a dramatically decrease in the mitochondrial bioenergetics in terms of reduced RCR and ADP/O in both the brain regions of AD-like rodents. Exendin-4 attenuated the Aβ-induced mitochondria dysfunction in addition to the decrease in the extent of phosphorylation of Akt in both the brain regions. In addition, PI3K inhibition abrogated the effects of Exendin-4 in AD-like animals. In support to our results, it has been reported that Exendin-4 protected beta cells from human islet amyloid polypeptide- and lipotoxicity-induced cell death partially through the activation of PI3K/Akt pathway and improved mitochondrial function (Fan et al., 2010; Wei et al., 2012). Additionally, Exendin-4 protected adipose-derived and bone marrow mesenchymal stem cell apoptosis through PI3K/Akt pathway (Zhou et al., 2014, 2015). The correlation analysis of the present study demonstrates the fact that the attributes of the mitochondrial dysfunction (MMP and RCR) of HIP and PFC were positively correlated to the loss in memory formation in the animals separately. Further, there was a negative correlation between mitochondrial dysfunction and the level of Aβ and activity of AChE in each brain regions of these rodents. Additionally, the mitochondrial dysfunction and the level of ACh and activity of ChAT were positively correlated in both the brain regions of these animals. These observations clearly demarcate the fact that Exendin-4 improves mitochondrial function in Aβ-induced AD-like animals perhaps through PI3K/Akt-

Table-1
Effect of E4 on Aβ-induced changes in the activities of mitochondrial complex enzyme-I, II, IV and V in rat HIP and PFC.

	Control	Sham	Aβ	Aβ+E4	Aβ+LY294002 + E4	Aβ+Donepezil
Complex-I (nmol NADH oxidized/min/mg protein)						
HIP	5.1 ± 0.5	5.3 ± 0.4	9.8 ± 0.7 ^{a,b}	6.9 ± 0.4 ^{a,b,c}	9.7 ± 0.5 ^{a,b,d}	7.1 ± 0.3 ^{a,b,c,e}
PFC	3.8 ± 0.7	4.1 ± 0.5	8.9 ± 0.6 ^{a,b}	6.8 ± 0.6 ^{a,b,c}	9.3 ± 0.4 ^{a,b,d}	6.8 ± 0.5 ^{a,b,c,e}
Complex-II (μmol formazan produced/min/mg protein)						
HIP	0.4 ± 0.02	0.4 ± 0.01	1.1 ± 0.02 ^{a,b}	1.1 ± 0.01 ^{a,b}	1.2 ± 0.01 ^{a,b}	1.2 ± 0.02 ^{a,b}
PFC	0.5 ± 0.03	0.4 ± 0.03	1.2 ± 0.02 ^{a,b}	1.2 ± 0.01 ^{a,b}	1.1 ± 0.01 ^{a,b}	1.1 ± 0.01 ^{a,b}
Complex-IV (nmol cytochrome *c* oxidized/min/mg protein)						
HIP	0.9 ± 0.03	0.8 ± 0.04	1.8 ± 0.03 ^{a,b}	1.3 ± 0.04 ^{a,b,c}	1.9 ± 0.02 ^{a,b,d}	1.4 ± 0.02 ^{a,b,c,e}
PFC	1.5 ± 0.02	1.3 ± 0.03	2.7 ± 0.04 ^{a,b}	1.9 ± 0.03 ^{a,b,c}	2.6 ± 0.03 ^{a,b,d}	1.8 ± 0.01 ^{a,b,c,e}
Complex-V (nmol ATP hydrolyzed/mg protein)						
HIP	7.5 ± 0.4	7.3 ± 0.5	15.3 ± 0.8 ^{a,b}	9.5 ± 0.4 ^{a,b,c}	15.2 ± 0.7 ^{a,b,d}	9.3 ± 0.5 ^{a,b,c,e}
PFC	12.5 ± 0.7	11.3 ± 0.6	23.3 ± 1.1 ^{a,b}	18.9 ± 1.1 ^{a,b,c}	24.1 ± 1.5 ^{a,b,d}	19.1 ± 0.9 ^{a,b,c,e}

All values are Mean ± SEM (n = 6). $^{a}P < 0.05$ compared to Control, $^{b}P < 0.05$ compared to Sham, $^{c}P < 0.05$ compared to Aβ, $^{d}P < 0.05$ compared to Aβ+E4 and $^{e}P < 0.05$ compared to Aβ+LY294002 + E4 (One-way ANOVA followed by Student Newmann Keuls Post hoc test).

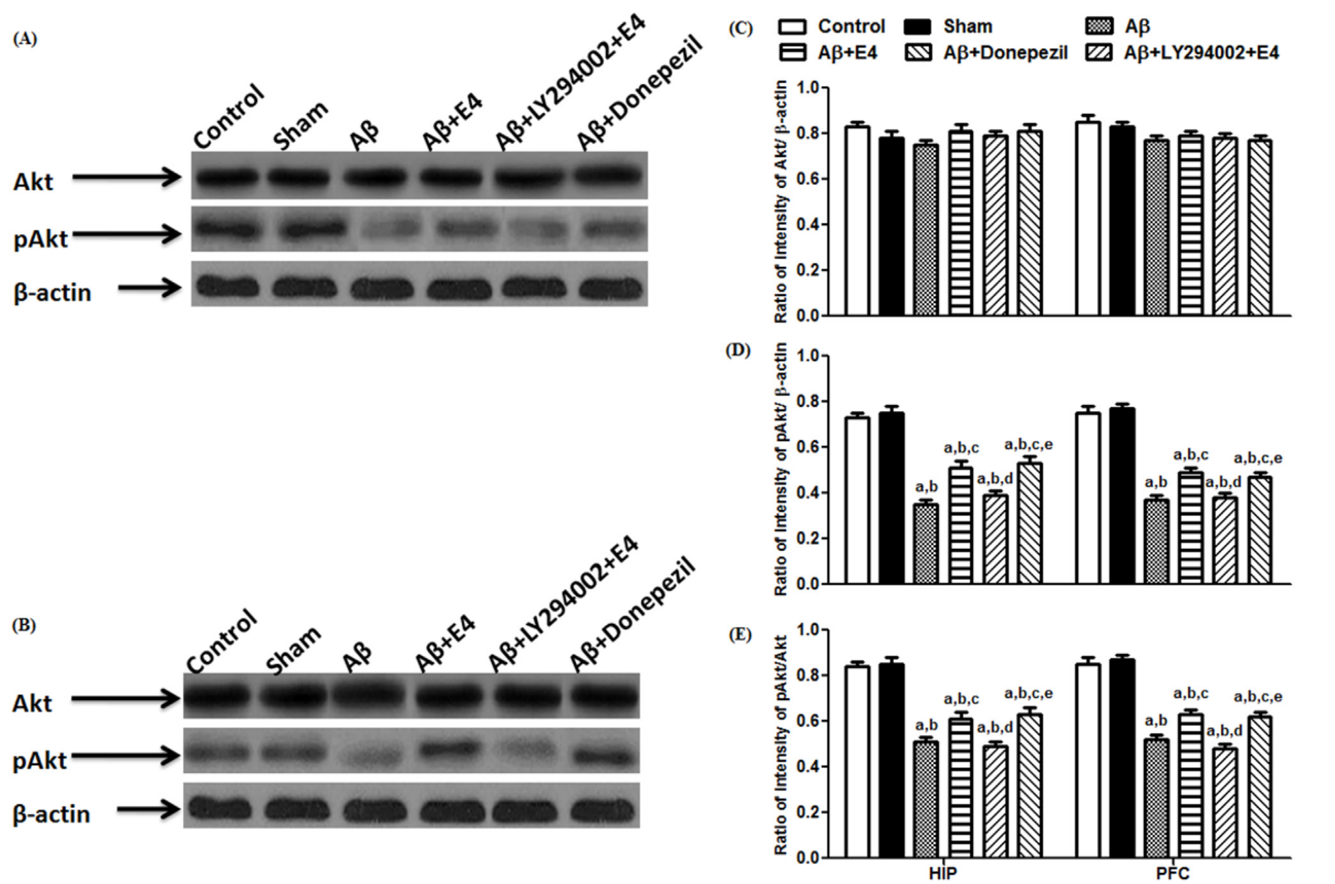

Fig. 10. The effect E4 on Aβ-induced changes in the levels of expression of Akt (C) and pAkt (D), and ratio of pAkt to Akt (E) in rat HIP and PFC. The blots are representative of Akt (A) and pAkt (B) in HIP and PFC. The results in the histogram are expressed as the ratio of relative intensity of levels of expression of Akt or pAkt to β-actin All values are Mean ± SEM (N = 6). $^{a}P < 0.05$ compared to Control, $^{b}P < 0.05$ compared to Sham, $^{c}P < 0.05$ compared to Aβ, $^{d}P < 0.05$ compared to Aβ + E4 and $^{e}P < 0.05$ compared to Aβ + LY294002 + E4 (One-way ANOVA followed by Student Newmann Keuls Post-hoc test).

Table-2

The results illustrate the correlation analysis between MMP and mitochondrial RCR of HIP and PFC and memory loss in MWM and Y-maze test protocol. Moreover, results reveal the correlation analysis between MMP and mitochondrial RCR, amyloid beta and cholinergic dysfunction in rat HIP and PFC.

Brain region & Mitochondrial parameter	Behavioral/Biochemical parameter	r^2	Pearson r	Slope
MMP of HIP	Time spent in target quadrant (Sec) in Morris water maze	0.93	0.96	0.28 ± 0.01
	Spontaneous alternation behavior (%) in Y-maze	0.95	0.97	0.25 ± 0.01
	Aβ	0.97	−0.99	−0.05 ± 0.001
	Acetylcholine	0.95	0.97	0.002 ± 0.00008
	Acetylcholinestarase activity	0.96	−0.98	−0.21 ± 0.007
	Choline acetyltransferase activity	0.97	0.98	0.003 ± 0.0001
RCR of HIP	Time spent in target quadrant (Sec) in Morris water maze	0.80	0.89	12.18 ± 1.05
	Spontaneous alternation behavior (%) in Y-maze	0.89	0.95	11.93 ± 0.70
	Aβ	0.94	−0.97	−2.25 ± 0.096
	Acetylcholine	0.95	0.98	0.09 ± 0.003
	Acetylcholinestarase activity	0.91	−0.95	−9.51 ± 0.51
	Choline acetyltransferase activity	0.93	0.96	0.15 ± 0.007
MMP of PFC	Time spent in target quadrant (Sec) in Morris water maze	0.93	0.96	0.28 ± 0.013
	Spontaneous alternation behavior (%) in Y-maze	0.97	0.98	0.27 ± 0.008
	Aβ	0.96	−0.98	−0.05 ± 0.0018
	Acetylcholine	0.94	0.97	0.002 ± 0.00009
	Acetylcholinestarase activity	0.96	−0.98	−0.21 ± 0.007
	Choline acetyltransferase activity	0.93	0.96	0.006 ± 0.0003
RCR of PFC	Time spent in target quadrant (Sec) in Morris water maze	0.8569	0.9257	10.96 ± 0.77
	Spontaneous alternation behavior (%) in Y-maze	0.9081	0.9529	10.45 ± 0.57
	Aβ	0.9546	−0.977	−1.98 ± 0.074
	Acetylcholine	0.8549	0.9246	0.076 ± 0.005
	Acetylcholinestarase activity	0.9293	−0.964	−8.35 ± 0.39
	Choline acetyltransferase activity	0.8461	0.9198	0.23 ± 0.02

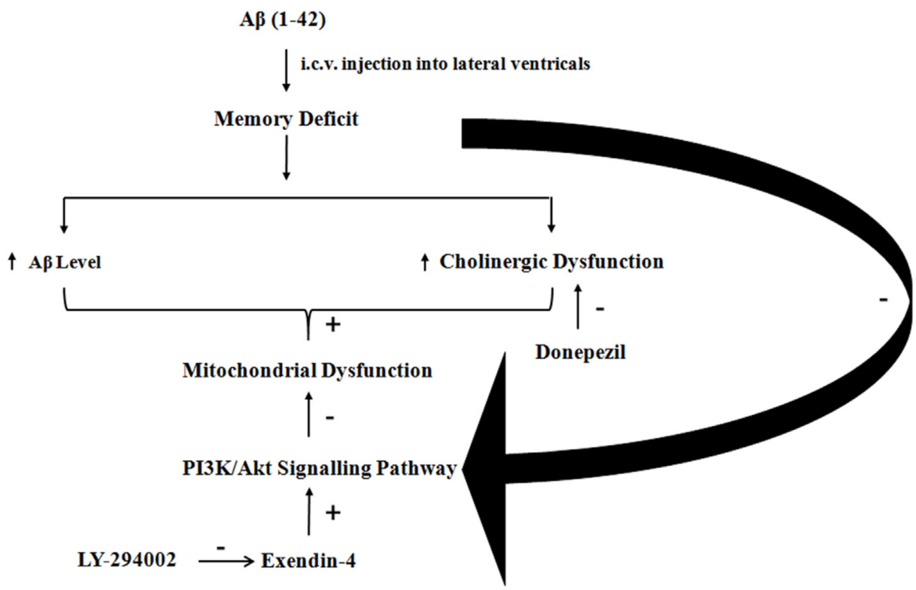

Fig. 11. Diagrammatic representation of the conclusion of the study. Briefly, intracerebroventricular administration of Aβ (1–42) caused cognitive deficits in male rats. Further, Aβ injection increased the level of Aβ and cholinergic dysfunction, and reduced the signaling of PI3K/Akt in all the rat brain regions. At the sub-cellular level, there was mitochondrial dysfunction in all the brain regions of the Aβ challenged rats. E4 significantly attenuated Aβ-induced aberration in behavioral, biochemical and molecular parameters in all the rat brain regions similar to that of Donepezil. However, LY-294002, PI3K inhibitor, diminished the therapeutic effects of E4 in AD-like animals indicating that E4 may mitigate AD-like manifestations perhaps through PI3K/Akt-mediated pathway in these animals. Thus, E4 could be a potential therapeutic alternative candidate in the management of AD.

mediated signaling pathway.

In conclusion, Exendin-4 attenuated mitochondrial toxicity in memory-sensitive brain regions of Aβ-induced AD-like rodents. In addition, Exendin-4 reduced Aβ level and cholinergic dysfunction in these regions of AD-like rats. However, LY-294002 abrogated the therapeutic effects of Exendin-4 against AD-like animals. Thus, it can be speculated that Exendin-4 may mitigate AD-like manifestations perhaps through PI3K/Akt-mediated pathway in the experimental animals (Fig-11). Hence, Exendin-4 could be a potential therapeutic alternative candidate in the management of AD.

Conflicts of interest

The authors declare that they have no conflict of interests.

Acknowledgments

JV is thankful to GLA University, Mathura, Uttar Pradesh, India for the financial assistantship.

References

Agis-Torres, A., Söllhuber, M., Fernandez, M., Sanchez-Montero, J.M., 2014. Multi-target directed ligands and other therapeutic strategies in the search of a real solution for Alzheimer's disease. Curr. Neuropharmacol. 12, 2–36.
Agostinho, P., Cunha, R.A., Oliveira, C., 2010. Neuro inflammation, oxidative stress and the pathogenesis of Alzheimer's disease. Curr. Pharmaceut. Des. 16, 2766–2778.
Athauda, D., Maclagan, K., Skene, S.S., Bajwa-Joseph, M., Letchford, D., Chowdhury, K., Hibbert, S., Budnik, N., Zampedri, L., Dickson, J., Li, Y., Aviles-Olmos, I., Warner, T.T., Limousin, P., Lees, A.J., Greig, N.H., Tebbs, S., Foltynie, T., 2017. Exenatide once weekly versus placebo in Parkinson's disease: a randomised, double-blind, placebo-controlled trial. Lancet 390, 1664–1675.
Benilova, I., Karran, E., De Strooper, B., 2012. The toxic Aβ oligomer and Alzheimer's disease: an emperor in need of clothes. Nat. Neurosci. 15, 349–357.
Bowen, D.M., Smith, C.B., White, P., Davison, A.N., 1976. Neurotransmitter-related enzymes and indices of hypoxia in senile dementia and other abiotrophies. Brain 99, 459–496.
Bradford, M.M., 1976. A rapid and sensitive method for the quantitation of microgram quantities of protein utilizing the principle of protein-dye binding. Anal. Biochem. 72, 248–254.
Bush, A.I., 2013. The metal theory of Alzheimer's disease. J. Alzheimer's Dis. 1, 277–281.
Chance, B., Williams, G.R., 1956. Respiratory enzymes in oxidative phosphorylation. VI. The effects of adenosine diphosphate on azide-treated mitochondria. J. Biol. Chem. 221, 477–489.
Chen, X., Hu, J., Jiang, L., Xu, S., Zheng, B., Wang, C., Zhang, J., Wei, X., Chang, L., Wang, Q., 2014. Brilliant blue g improves cognition in an animal model of Alzheimer's disease and inhibits amyloid-beta-induced loss of filopodia and dendrite spines in hippocampal neurons. Neuroscience 279, 94–101.
Darsalia, V., Mansouri, S., Ortsäter, H., Olverling, A., Nozadze, N., Kappe, C., Iverfeldt, K., Tracy, L.M., Grankvist, N., Sjöholm, Å., Patrone, C., 2012. Glucagon-like peptide-1 receptor activation reduces ischaemic brain damage following stroke in Type 2 diabetic rats. Clin. Sci. 122, 473–483.
Devi, L., Prabhu, B.M., Galati, D.F., Avadhani, N.G., Anandatheerthavarada, H.K., 2006. Accumulation of amyloid precursor protein in the mitochondrial import channels of human Alzheimer's disease brain is associated with mitochondrial dysfunction. J. Neurosci. 26, 9057–9068.
Dragicevic, N., Copes, N., O'Neal-Moffitt, G., Jin, J., Buzzeo, R., Mamcarz, M., Tan, J., Cao, C., Olcese, J.M., Arendash, G.W., Bradshaw, P.C., 2011. Melatonin treatment restores mitochondrial function in Alzheimer's mice: a mitochondrial protective role of melatonin membrane receptor signaling. J. Pineal Res. 51, 75–86.
Du, H., Guo, L., Fang, F., Chen, D., Sosunov, A.A., McKhann, G.M., Yan, Y., Wang, C., Zhang, H., Molkentin, J.D., Gunn-Moore, F.J., Vonsattel, J.P., Arancio, O., Chen, J.X., Yan, S.D., 2008. Cyclophilin D deficiency attenuates mitochondrial and neuronal perturbation and ameliorates learning and memory in Alzheimer's disease. Nat. Med. 14 1097-1095.
Eissa, N., Khan, N., Ojha, S.K., Łazewska, D., Kieć-Kononowicz, K., Sadek, B., 2018. The histamine H3 receptor antagonist DL77 ameliorates MK801-induced memory deficits in rats. Front. Neurosci. 12, 12–42.
Fan, R., Li, X., Gu, X., Chan, J.C., Xu, G., 2010. Exendin-4 protects pancreatic beta cells from human islet amyloid polypeptide-induced cell damage: potential involvement of AKT and mitochondria biogenesis. Diabetes Obes. Metab. 12, 815–824.
Fiske, C.H., Subbarao, Y., 1925. The colorimetric determination of phosphorus. J. Biol. Chem. 66, 375–400.
Francis, P.T., Palmer, A.M., Snape, M., Wilcock, G.K., 1999. The cholinergic hypothesis of Alzheimer's disease: a review of progress. J. Neurol. Neurosurg. Psychiatry 66, 137–147.
Giacobini, E., Gold, G., 2013. Alzheimer disease therapy–moving from amyloid-β to tau. Nat. Rev. Neurol. 9, 677–686.
Goure, W.F., Krafft, G.A., Jerecic, J., Hefti, F., 2014. Targeting the proper amyloid-beta neuronal toxins: a path forward for Alzheimer's disease immunotherapeutics. Alzheimer's Res. Ther. 6, 42.
Griffiths, D.E., Houghton, R.L., 1974. Studies on energy linked reactions: modified mitochondrial ATPase of oligomycin-resistant mutants of Saccharomyces cerevisiae. Eur. J. Biochem. 46, 157–167.
Grimaldi, M., Marino, S.Di, Florenzano, F., Ciotta, M.T., Nori, S.L., Rodriquez, M., Sorrentino, G., D'Ursi, A.M., Scrima, M., 2016. β-Amyloid-acetylcholine molecular interaction: new role of cholinergic mediators in anti-Alzheimer therapy? Future Med. Chem. 8, 1179–1189.
Hoshi, M., Takashima, A., Murayama, M., Yasutake, K., Yoshida, N., Ishiguro, K., Hoshino, T., Imahori, K., 1997. Nontoxic amyloid beta peptide 1-42 suppresses acetylcholine synthesis. Possible role in cholinergic dysfunction in Alzheimer's disease. J. Biol. Chem. 272, 2038–2041.
Huang, S.G., 2002. Development of a high throughput screening assay for mitochondrial membrane potential in living cells. J. Biomol. Screen 7, 383–389.
Jia, X.T., Ye-Tian, Yuan-Li, Zhang, G.J., Liu, Z.Q., Di, Z.L., Ying, X.P., Fang, Y., Song, E.F., Qi, J.S., Pan, Y.F., 2016. Exendin-4, a glucagon-like peptide 1 receptor agonist, protects against amyloid-β peptide-induced impairment of spatial learning and memory in rats. Physiol. Behav. 159, 72–79.
Kamboj, S.S., Kumar, V., Kamboj, A., Sandhir, R., 2008. Mitochondrial oxidative stress and dysfunction in rat brain induced by carbofuran exposure. Cell. Mol. Neurobiol. 28, 961–969.
Karran, E., Mercken, M., De Strooper, B., 2011. The amyloid cascade hypothesis for Alzheimer's disease: an appraisal for the development of therapeutics. Nat. Rev. 10, 698–712.
Lambert, M.P., Barlow, A.K., Chromy, B.A., Edwards, C., Freed, R., Liosatos, M., Morgan,

T.E., Rozovsky, I., Trommer, B., Viola, K.L., Wals, P., Zhang, C., Finch, C.E., Krafft, G.A., Klein, W.L., 1998. Diffusible, nonfibrillar ligands derived from Abeta1-42 are potent central nervous system neurotoxins. Proc. Natl. Acad. Sci. U.S.A. 95, 6448–6453.

Li, Y., Duffy, K.B., Ottinger, M.A., Ray, B., Bailey, J.A., Holloway, H.W., Tweedie, D., Perry, T., Mattson, M.P., Kapogiannis, D., Sambamurti, K., Lahiri, D.K., Greig, N.H., 2010. GLP-1 receptor stimulation reduces amyloid-beta peptide accumulation and cytotoxicity in cellular and animal models of Alzheimer's disease. J. Alzheimer's Dis. 19, 1205–1219.

Li, X., Zhao, X., Xu, X., Mao, X., Liu, Z., Li, H., Guo, L., Bi, K., Jia, Y., 2014. Schisantherin A recovers Aβ-induced neurodegeneration with cognitive decline in mice. Physiol. Behav. 132, 10–16.

Lin, H.B., Yang, X.M., Li, T.J., Cheng, Y.F., Zhang, H.T., Xu, J.P., 2009. Memory deficits and neurochemical changes induced by C-reactive protein in rats: implication in Alzheimer's disease. Psychopharmacology 204, 705–714.

Liu, M., Kay, J.C., Shen, S., Qiao, L.Y., 2015. Endogenous BDNF augments NMDA receptor phosphorylation in the spinal cord via PLCγ, PKC, and PI3K/Akt pathways during colitis. J. Neuroinflammation 12, 151.

Lowry, O.H., Rosenborough, N.J., Farr, A.L., Randall, R.J., 1951. Protein measurement with folin phenol reagent. J. Biol. Chem. 193, 265–275.

Mangialasche, F., Solomon, A., Winblad, B., Mecocci, P., Kivipelto, M., 2010. Alzheimer's disease: clinical trials and drug development. Lancet Neurol. 9, 702–716.

Mattson, M.P., 2010. ER calcium and Alzheimer's disease: in a state of flux. Sci. Signal. 3, 10.

McClean, P.L., Parthsarathy, V., Faivre, E., Hölscher, C., 2011. The diabetes drug liraglutide prevents degenerative processes in a mouse model of Alzheimer's disease. J. Neurosci. 31, 6587–6594.

Morris, R., 1984. Developments of a water-maze procedure for studying spatial learning in the rat. J. Neurosci. Methods 11, 47–60.

Mouri, A., Noda, Y., Hara, H., Mizoguchi, H., Tabira, T., Nabeshima, T., 2007. Oral vaccination with a viral vector containing Aβ cDNA attenuates age-related Aβ accumulation and memory deficits without causing inflammation in a mouse Alzheimer model. FASEB J. 21, 2135–2148.

Muthuraju, S., Maiti, P., Solanki, P., Sharma, A.K., Amitabh Singh, S.B., Prasad, D., Ilavazhagan, G., 2009. Acetylcholinesterase inhibitors enhance cognitive functions in rats following hypobaric hypoxia. Behav. Brain Res. 203, 1–14.

National Research Council (US) Committee for the Update of the Guide for the Care and Use of Laboratory Animals (2011) Guide for the Care and Use of Laboratory Animals, eighth ed. National Academies Press (US), Washington, DC.

Nillert, N., Pannangrong, W., Welbat, J., Chaijaroonkhanarak, W., Sripanidkulchai, K., Sripanidkulchai, B., 2017. Neuroprotective effects of aged garlic extract on cognitive dysfunction and neuroinflammation induced by β-amyloid in rats. Nutrients 9, E24.

Onyango, I.G., 2018. Modulation of mitochondrial bioenergetics as a therapeutic strategy in Alzheimer's disease. Neural Regen. Res. 13, 19–25.

Pandey, S., Garabadu, D., 2017. Piracetam facilitates the anti-amnesic but not anti-diabetic activity of metformin in experimentally induced type-2 diabetic encephalopathic rats. Cell. Mol. Neurobiol. 37, 791–802.

Patterson, C., 2018. World Alzheimer Report 2018: the State of the Art of Dementia Research: New Frontiers. Alzheimer’s Disease International, 2018, London.

Paxinos, G., Watson, C. (Eds.), 1998. The Rat Brain in Stereotaxic Coordinates. Acad Press, New York, pp. 4.

Pedersen, P.L., Greenawalt, J.W., Reynafarje, B., Hullihen, J., Decker, G.L., Soper, J.W., Bustamente, E., 1978. Preparation and characterization of mitochondria and submitochondrial particles of rat liver-derived tissues. Methods Cell Biol. 20, 411–481.

Perry, T., Lahiri, D.K., Sambamurti, K., Chen, D., Mattson, M.P., Egan, J.M., Greig, N.H., 2003. Glucagon-like peptide-1 decreases endogenous amyloid-beta peptide (Abeta) levels and protects hippocampal neurons from death induced by Abeta and iron. J. Neurosci. Res. 72, 603–612.

Perry, T.A., Greig, N.H., 2004. A new Alzheimer's disease interventive strategy: GLP-1. Curr. Drug Targets 5, 565–571.

Reddy, P.H., Reddy, T.P., 2011. Mitochondria as a therapeutic target for aging and neurodegenerative diseases. Curr. Alzheimer Res. 8, 393–409.

Sally, L.O., Margaret, A.J., 1989. Methods of microphotometric assay of succinate dehydrogenase and cytochrome-C oxidase activities for use on human skeletal muscle. Histochem. J. 21, 545–555.

Shapiro, B.L., Feigal, R.J., Lam, F.H., 1979. Mitochondrial NADH dehydrogenase in cystic fibrosis. Proc. Natl. Acad. Sci. U.S.A. 76, 2979–2983.

Šimić, G., Babić Leko, M., Wray, S., Harrington, C., Delalle, I., Jovanov-Milošević, N., Bažadona, D., Buée, L., de Silva, R., Di Giovanni, G., Wischik, C., Hof, P.R., 2016. Tau protein hyperphosphorylation and aggregation in alzheimer's disease and other tauopathies, and possible neuroprotective strategies. Biomolecules 6, 6.

Simoncini, C., Orsucci, D., Caldarazzo, E., Siciliano, G., Bonuccelli, U., Mancuso, M., 2015. Alzheimer's pathogenesis and its link to the mitochondrion. Oxid. Med. Cell Longev. 2015, 803942.

Storrie, B., Madden, E.A., 1990. Isolation of subcellular organelles. Methods Enzymol. 182, 203–225.

Summers, W.K., Majovski, L.V., Marsh, G.M., Tachiki, K., Kling, A., 1986. Oral tetrahydroaminoacridine in long-term treatment of senile dementia, Alzheimer type. N. Engl. J. Med. 315, 1241–1245.

Swerdlow, R.H., Burns, J.M., Khan, S.M., 2010. The Alzheimer's disease mitochondrial cascade hypothesis. J. Alzheimer's Dis. 20, S265–S279.

Wang, X., Wang, L., Jiang, R., Xu, Y., Zhao, X., Li, Y., 2016. Exendin-4 antagonizes Aβ1-42-induced attenuation of spatial learning and memory ability. Exp. Ther. Med. 12, 2885–2892.

Wei, Q., Sun, Y.Q., Zhang, J., 2012. Exendin-4, a glucagon-like peptide-1 receptor agonist, inhibits cell apoptosis induced by lipotoxicity in pancreatic β-cell line. Peptides 37, 18–24.

Whitehouse, P.J., Price, D.L., Clark, A.W., Coyle, J.T., DeLong, M.R., 1981. Alzheimer disease: evidence for selective loss of cholinergic neurons in the nucleus basalis. Ann. Neurol. 10, 122–126.

Yan, Z., Feng, J., 2004. Alzheimer's disease: interactions between cholinergic functions and beta-amyloid. Curr. Alzheimer Res. 1, 241–248.

Ye, C.Y., Lei, Y., Tang, X.C., Zhang, H.Y., 2015. Donepezil attenuates Aβ-associated mitochondrial dysfunction and reduces mitochondrial Aβ accumulation in vivo and in vitro. Neuropharmacology 95, 29–36.

Zhou, H., Li, D., Shi, C., Xin, T., Yang, J., Zhou, Y., Hu, S., Tian, F., Wang, J., Chen, Y., 2015. Effects of Exendin-4 on bone marrow mesenchymal stem cell proliferation, migration and apoptosis in vitro. Sci. Rep. 7, 12898.

Zhou, H., Yang, J., Xin, T., Li, D., Guo, J., Hu, S., Zhou, S., Zhang, T., Zhang, Y., Han, T., Chen, Y., 2014. Exendin-4 protects adipose-derived mesenchymal stem cells from apoptosis induced by hydrogen peroxide through the PI3K/Akt-Sfrp2 pathways. Free Radic. Biol. Med. 77, 363–375.

Zoukhri, D., Kublin, C.L., 2001. Impaired neurotransmitter release from lacrimal and salivary gland nerves of a murine model of sjögren's syndrome. Investig. Ophthalmol. Vis. Sci. 42, 925–932.